ORIGINAL ARTICLE

BUEVA: a bi-directional ultrasonic elliptical vibration actuator for micromachining

Ali H. Ammouri · Ramsey F. Hamade

Abstract This paper presents a novel actuator design for vibration-induced micromachining. The bi-directional ultrasonic elliptical vibration actuator (BUEVA) possesses a combination of features that renders it suitable for the machining a wide range of materials over a variety of cutting parameters. The cutting motion is an elliptical tool motion that resembles "spoon feeding". This cutting action is in contrast to in-plane, horizontal motion utilized by most existing setups. The motion is arrived at through a combination of motions along the tool's axial and transverse directions and by vibrating out of phase and is generated by two stacked ceramic multilayer actuator ring piezo elements. Another distinguishing feature of BUEVA is the use of piezo stacks which ensure high blocking force compared to low force of piezo benders as used in many existing actuators. Furthermore, the amplitude and frequency of vibration of the tool are controlled on-line in order to vary the cutting depth and cutting speed according to the desired cutting parameters. This is a desirable characteristic which allows one to "dial-in" a desirable cutting speed for different workpiece materials. Another attractive BUEVA feature is that the design is very compact and can fit easily into the working space of most milling machining centers without the need for custom motion setups. An off the shelf TiALN-coated carbide turning tool is utilized as the cutting tool. Furthermore, refined versions of previously reported models by other workers in the micromachining field have been developed. Experimental force and surface roughness measurements are compared versus these ideal calculations from the improved models. Compared with these reference models, our refined calculations show improvements in describing chip geometry based on corrected tool motion and which, consequently, resulted in improved estimates of both surface roughness and cutting forces. Verification cutting tests in two different materials (Al2024 and Plexiglas) show good surface integrity and dimensional definition with roughness measurements in reasonable correlation to the refined model calculations.

Keywords Elliptical vibration cutting · Micromachining · Cutting forces · Surface roughness

1 Introduction

Vibration-assisted machining (VAM) and vibration-induced machining (VIM) have witnessed several developments since the introduction of these technologies in the early 1980s. VAM and VIM applications are quite varied [1–3]. In VAM the former, traditional tools do the cutting while being "assisted" by vibrations from external source. Vibration-induced machining, on the other hand, refers to tools that perform the actual cutting by virtue of their own vibration. However, it was not until the early 1990s when many different VAM and VIM designs were introduced which varied in the manner the vibration was induced, the plane of tool vibration, the operating frequency of the tool/work, and the degrees of freedom that the actuator possessed.

In VIM, tool variations include unidirectional [4–7] and bi-directional [8–18] motions with different bi-directional designs varying in the manner of achieving their elliptical cutting path: in-plane horizontal motion [10–12], in-plane vertical motion [13, 16–18], or 3DOF motion [14, 15].

A. H. Ammouri · R. F. Hamade (✉)
Department of Mechanical Engineering,
American University of Beirut,
Beirut 1107 2020, Lebanon
e-mail: rh13@aub.edu.lb

In addition to the cutting motion, the actuating force creation has been the source of a great variety as well. While many existing VIM designs use piezo-plate benders [13–15] that are known to have a very low blocking force, others use designs which incorporate piezo stacks [11, 16, 17]. Utilizing piezo-plate benders has the disadvantage of potentially creating undesirable deformation of the planned path especially if cutting at low speeds with open-loop control.

VIM actuators are further classified according to their operating frequency. Designs that require the tool to vibrate at a constant resonance frequency [4, 5, 13–16] lack the option to vary their cutting speed and thus are used to cut specific materials only. On the other hand, designs with the option to vibrate at any desired frequency offer flexibility to adapt the cutting speed according to the material being cut as originally [19] implemented by the setup developed in this work, bi-directional ultrasonic elliptical vibration actuator (BUEVA). More recently, several designs have adopted this design feature since [20, 21].

2 BUEVA's distinguishing features

BUEVA, being a vertical actuator, utilizes an elliptical vertical motion induced by two stacked ceramic multilayer actuator ring (SCMAR) with high blocking force. One stack vibrates in the tool's axial direction (the axial actuator) while the other vibrates transverse to the tool's axis (the transverse actuator, TA). The out-of-phase vibrations in the tool's transverse and axial directions cause the tool to vibrate elliptically in the plane of the actuator with the resulting motion resembling "spoon feeding" that can be found in similar tool designs [17–22].

In comparison with existing setups, BUEVA's combination of distinguishing design features is:

1. The ability to change the vibration frequency of the BUEVA on-line during cutting, as compared to fixed cutting speeds of other available actuators that vibrate at fixed resonant frequencies [4, 5, 13–16], makes it suitable to cut different materials according to the recommended cutting speed. Newly designed actuators [21] use a similar design approach.
2. The use of properly controlled high blocking force SCMARs, compared to the use of plate benders [13–15], guarantees that the tool vibrates according to the desired path. Some earlier designs [10] as well as more recent ones [20, 21] use stacked actuators to accomplish similarly good performance.
3. BUEVA's vertical operating position makes it easy to fit into any precision machining center without any
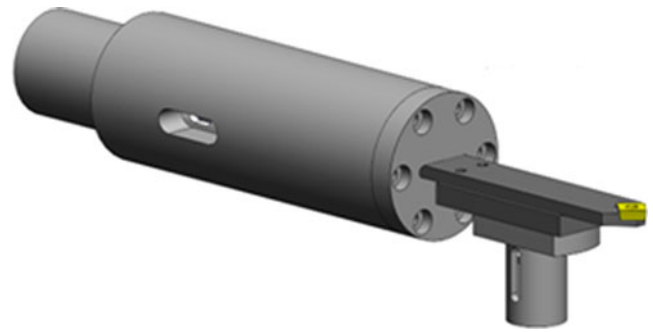
Fig. 1 A solid model of BUEVA (shown fully assembled)

special setup that is required by most existing actuator designs [8–18].
4. The utilization of an off the shelf TiALN-coated carbide (for lathe cutting) tool is another unique feature of BUEVA not found in other designs that operate on milling-like machines [14, 16, 20, 21]. This special feature makes tool-changing easy and no special tool design is required.

The combination of the above features makes BUEVA a novel VIM actuator that can be used to cut a variety of materials with ease and without the need of a special tool–workpiece setup. Figure 1 is a solid model representation of a fully assembled BUEVA.

2.1 Transverse motion

The transverse tool motion is a function of two parameters: the transverse vibration of the tool and the feed (linear) rate. The TA SCMAR is actuated by a sinusoidal signal supplied by the controller so the motion of the transverse actuator is also sinusoidal. The transverse actuator is shown in Fig. 2.

The motion of the SCMAR is transported to the tool holder by the plunger. The transverse actuator cover is used
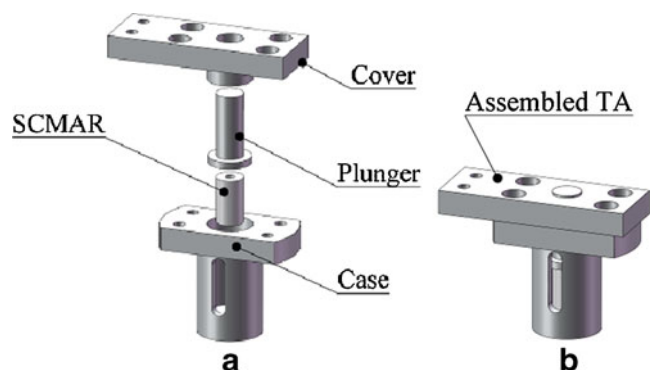
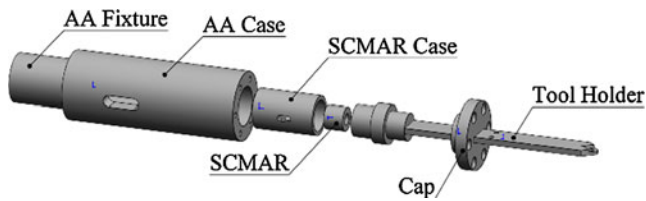Fig. 2 Transverse actuator exploded (**a**) and assembled (**b**) views

Fig. 3 Axial Actuator (*AA*) (Exploded view)

to attach it to the tool holder. Therefore, the total motion of the tool is described by

$$x = A \sin(2\pi f t) + f \times t \qquad (1)$$

Where x is the displacement of the tool in the transverse direction, A is the amplitude of vibration, f is the vibration frequency, and f is the tool feed.
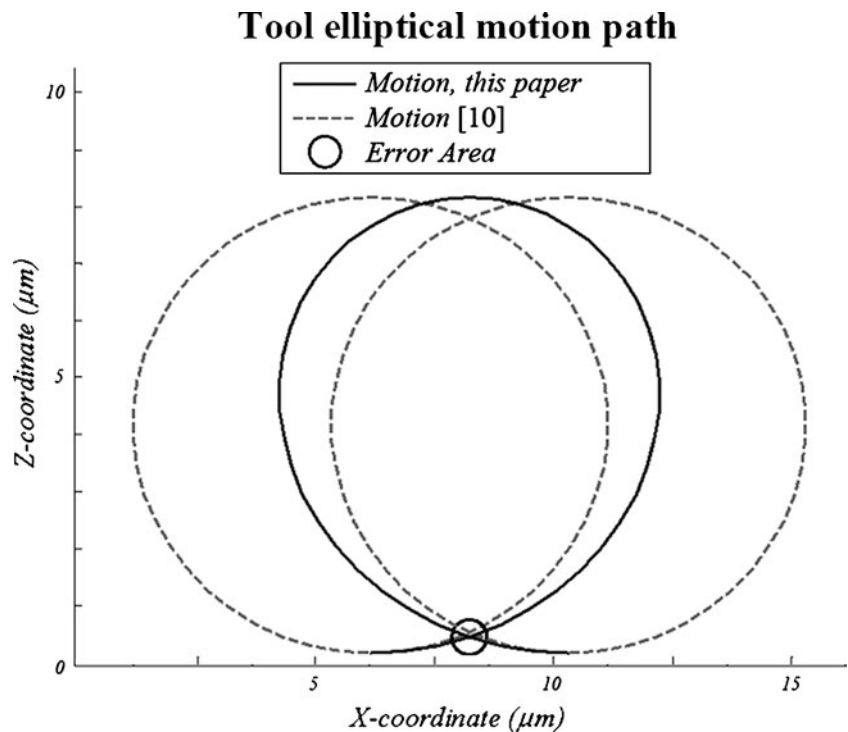
2.2 Axial actuator

The axial actuator of BUEVA (Fig. 3) is responsible for generating the axial motion of the tool that is the major contributor to the thrust force.

The signal delivered to the axial SCMAR is a sine wave 90° out of phase from that of the transverse SCMAR. The equation governing its motion in the axial plane is

$$z = -B \cos(2\pi f t) \qquad (2)$$

Where B is the amplitude of vibration of the axial SCMAR and f is the frequency of vibration of the transverse actuator. The negative sign indicates a downward movement when the cosine value is positive.

The combination of the sinusoidal motions of both the transverse and axial actuators will result in an elliptical path of the tool tip.

2.3 Chip formation

Accurate chip geometry should be modeled so that the cutting forces and the resulting surface finish can be accurately calculated. Cerniway [10] approximated the elliptical motion by a series of overlapping ellipses separated by distance equal to the feed. A more accurate model was developed in this work for more precise calculated estimates of the cutting forces and the generated surface finish. Figure 4 illustrates the source of error as the ideal ellipse deviates slightly from the actual motion.

To overcome this problem and model the actual motion precisely, a MATLAB script is used to generate an accurate model of the chip shape and size. The shape of the chips generated by BUEVA starts from zero at first engagement with the work and gradually increases to a maximum value at the intersection with the profile of the previous cut and then decreases steeply back to zero as it disengages from the workpiece. During a complete cutting cycle, the width of the chip is defined solely by the tip of the cutting tool (nose radius).

Fig. 4 Moving ellipse model error

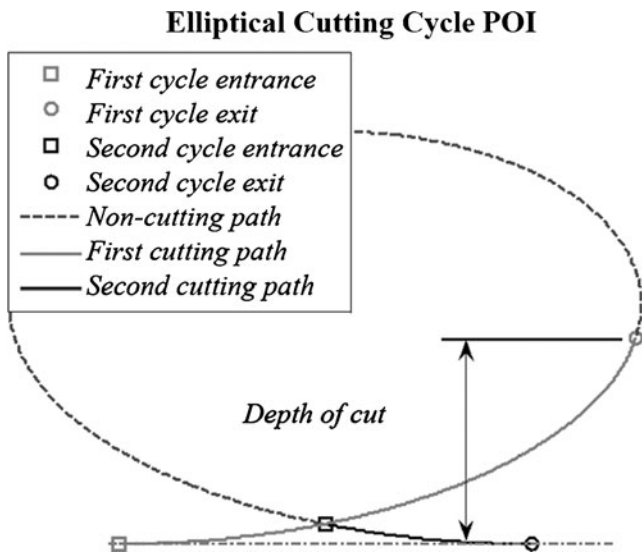## Elliptical Cutting Cycle POI

Fig. 5 Elliptical cutting cycle showing the points of interest (POIs)

A typical cutting cycle that shows the entrance and exit of the tool/workpiece engagement along with other points of interest is illustrated in Fig. 5. (The effect of this engagement will be clearly noticed in Section 4 below in improved estimates of the magnitude and profile of the cutting force generated as well as in the surface roughness produced).

2.4 Surface roughness

Also, surface roughness is function of the chip shape and geometry which depends on: the transverse and axial vibration amplitudes, frequency of these vibrations, and
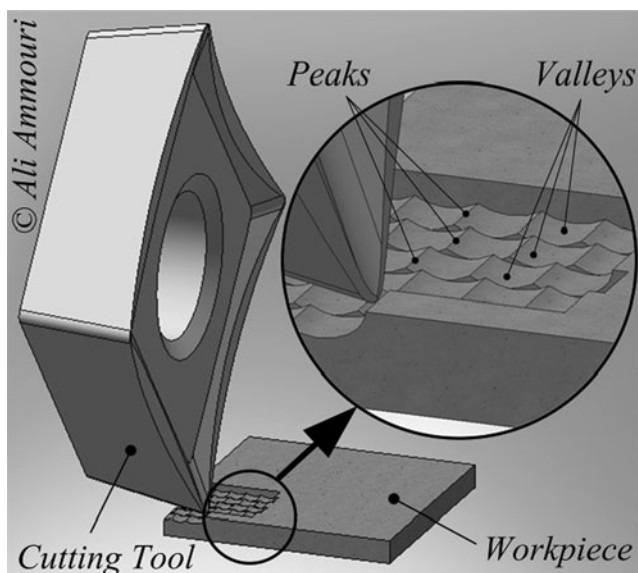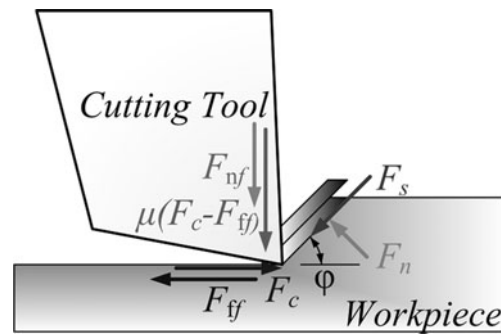

Fig. 6 BUEVA un-interlacing consecutive cuts

Fig. 7 Cutting force model (based on [22])

inline feed rate. It should be noted that the nature of the resulting cut suggests that the consecutive cutting paths to be un-interlacing (as shown in Fig. 6).

2.5 Cutting forces

We utilize the cutting forces model as introduced by Arcona [22] where the cutting force is calculated from the balance of forces between the tool and chip (Fig. 7) as it is being formed (but still attached to the workpiece).

The cutting and thrust components of the force are presented in Eqs. 3 and 4 and are function of the work's Brinell hardness (H) and modulus of elasticity (E), shear plane angle (φ), coefficients of friction on the rake (μ) and flank (μ_f) faces, and the contact areas between the tool and the work.

$$F_c = \frac{HA_c}{3}\left(\frac{\cot(\varphi)}{\sqrt{3}} + 1\right) + \mu_f A_f \times \left(0.62H\sqrt{\frac{43H}{E}}\right) \quad (3)$$

$$F_t = \mu\left[\frac{HA_c}{3}\left(\frac{\cot(\varphi)}{\sqrt{3}} + 1\right)\right] + A_f \times \left(0.62H\sqrt{\frac{43H}{E}}\right) \quad (4)$$

The above equations [22] are used to calculate the theoretical cutting forces for the different cutting tests in the validation of BUEVA.
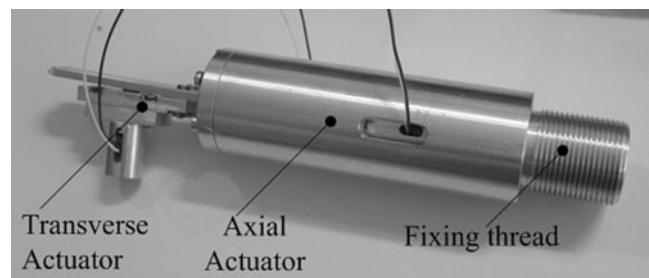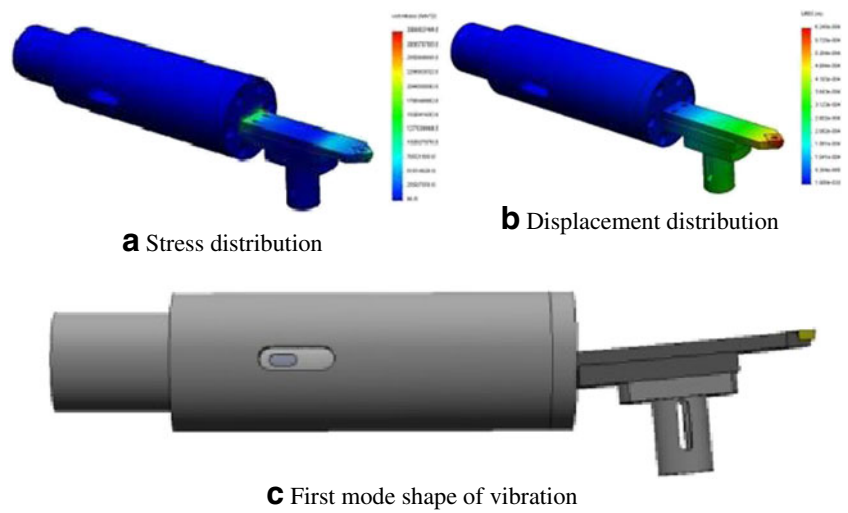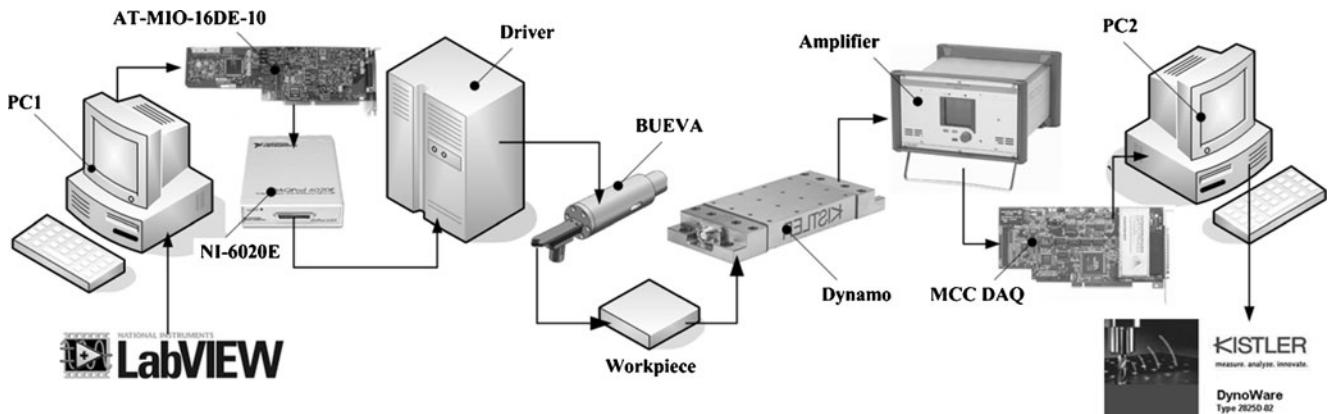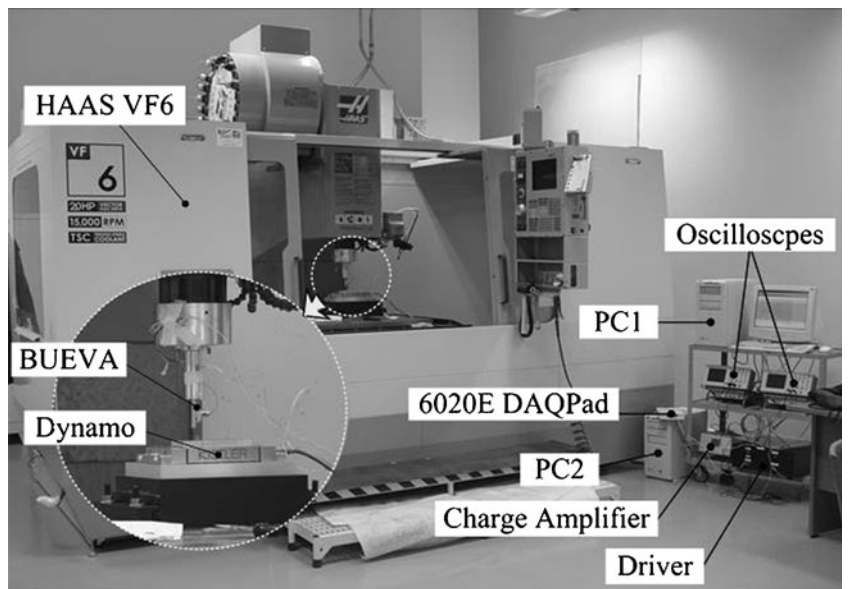

Fig. 8 Assembled BUEVA

Fig. 9 Mechanical simulations of BUEVA. **a** Stress distribution. **b** Displacement distribution. **c** First mode shape of vibration

a Stress distribution

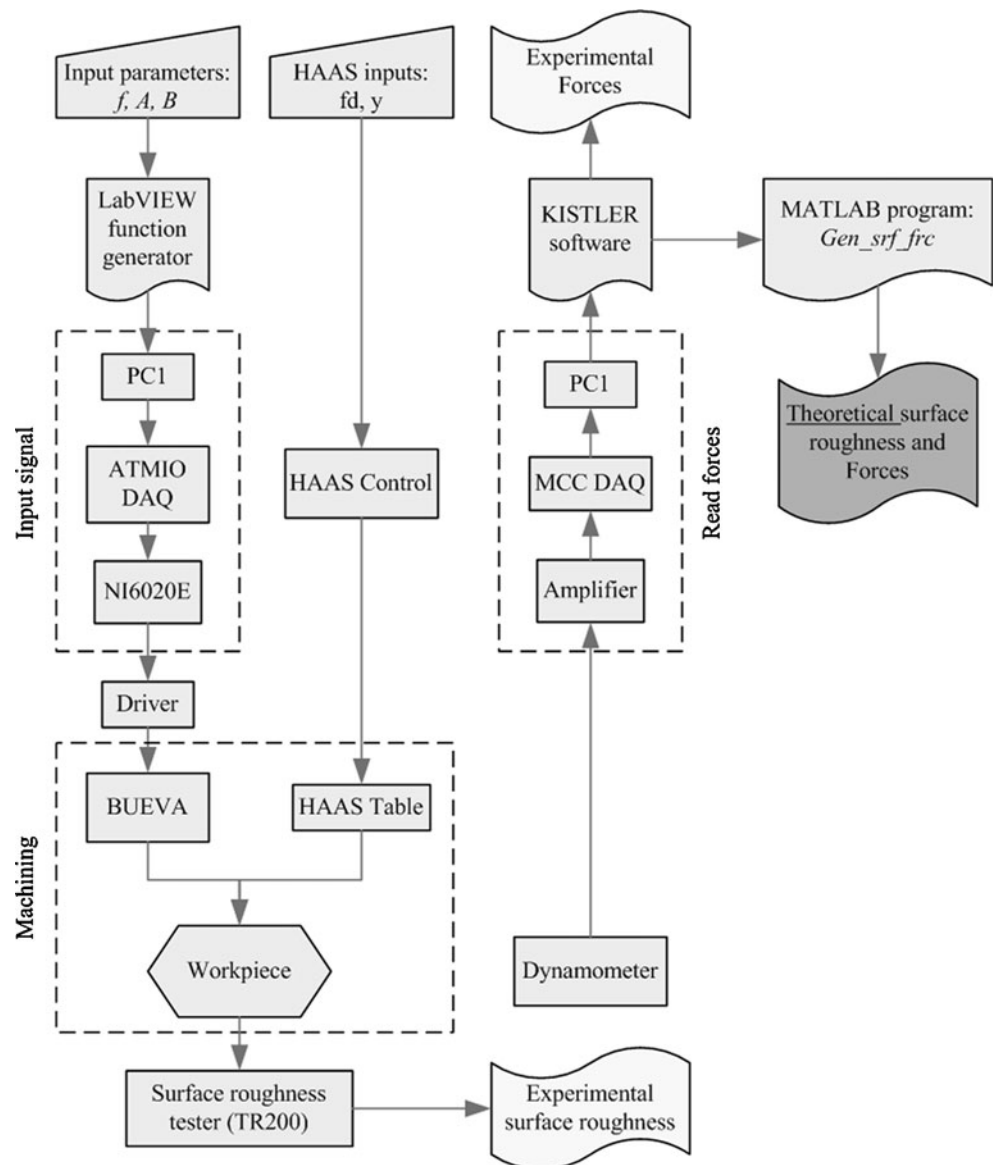**b** Displacement distribution

c First mode shape of vibration

Fig.10 The complete BUEVA Setup shown installed on Haas 6 vertical machining center

Fig. 11 The connectivity of the various modules and components of the BUEVA setup

Fig. 12 A flowchart diagram which illustrates the BUEVA system's flow of inputs and outputs as well as the overall scheme

Table 1 General BUEVA specifications (operating parameters)

Property	Value	Unit
Axial amplitude	1–30	μm
Transverse amplitude	1–10	μm
Frequency range	10–100,000	Hz
Overall length	196	mm
Overall width	47	mm
Overall depth	35	mm
Weight	350	g

40x magnification
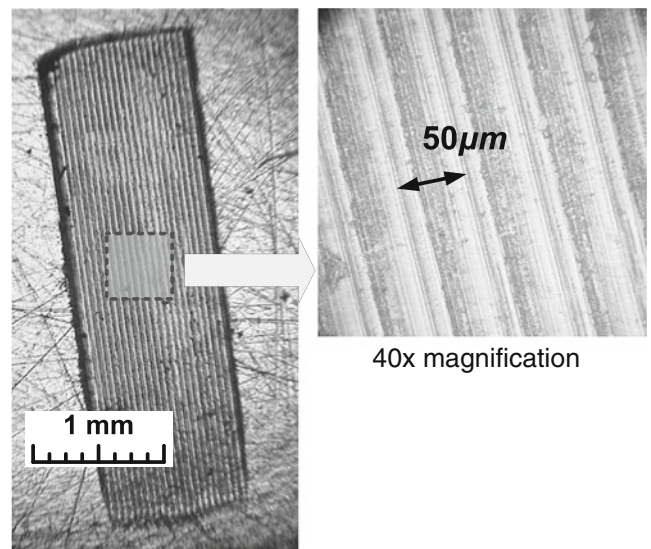
Fig. 13 Flat surface cut in AL2024

Fig. 14 Crossfeed surfaces roughness in AL 2024 work-piece (screenshot from AMBiOS XP1 profilometer)
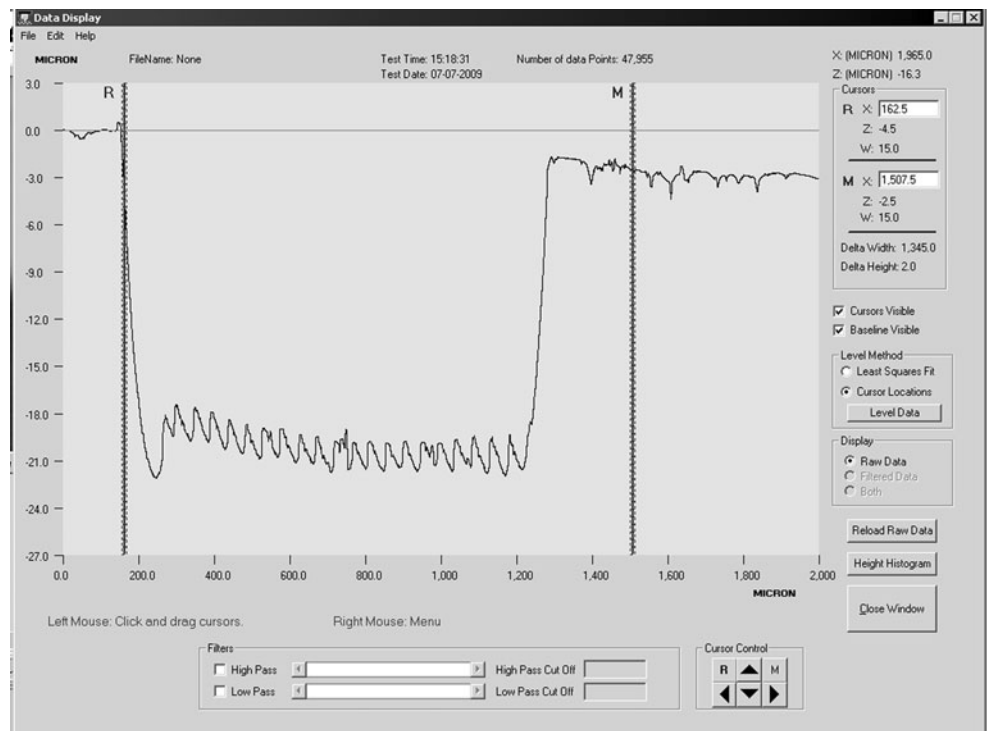
## 3 BUEVA system description

3.1 Implementation

The transverse (Fig. 2) and axial (Fig. 3) actuators were fabricated using Aluminum Alloy 2024. A photograph of the fully assembled BUEVA actuator is shown in Fig. 8.

The stresses and deformations predicted to occur in the assembled actuator were simulated and the results are shown in Fig. 9a and b. The first mode of vibration is estimated to occur at about 900 Hz (Fig. 9c) which is quite acceptable considering that BUEVA operates at frequencies of about 100 Hz.

3.2 Setup and control

The SCMAR requires high driving sinusoidal voltage with variable frequency and amplitude control. These control requirements were satisfied by building a BUEVA driver which takes a small control signal from a DAQ of a PC and amplifies it 20-fold to get the required driving voltage. The control signals fed to the SCMARs are generated from a program developed on LABVIEW. Two output channels are used on the DAQ to communicate with the amplifiers of the driver. The BUEVA driver takes a 220-VAC supply input and two transformers are used to step down the voltage to ±130 V. This voltage is transformed to DC by a full bridge circuit and

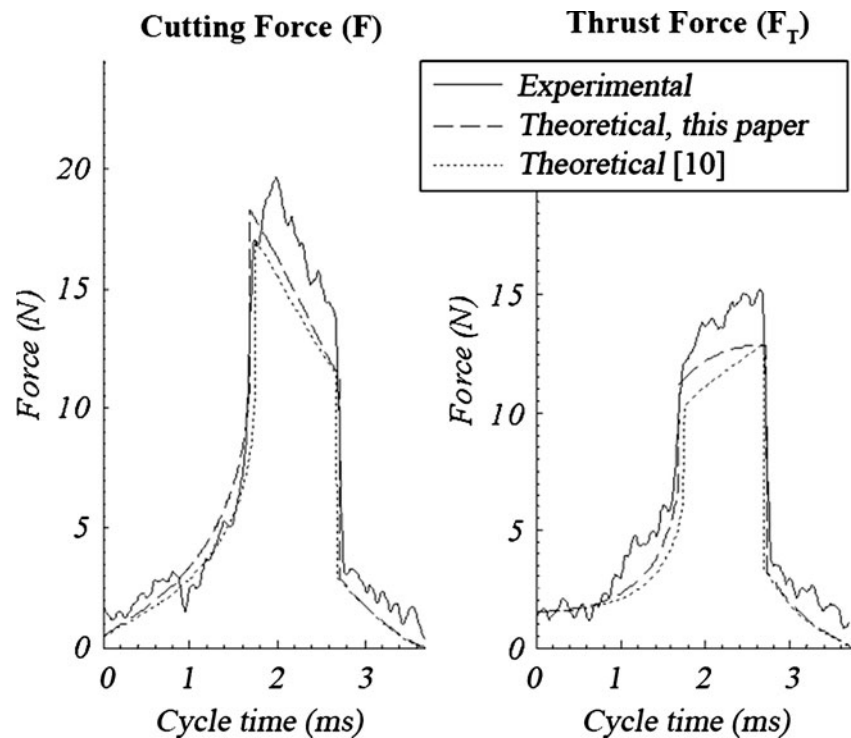**Fig. 15** Groove patterns corresponding to Table 2 (in AL2024)
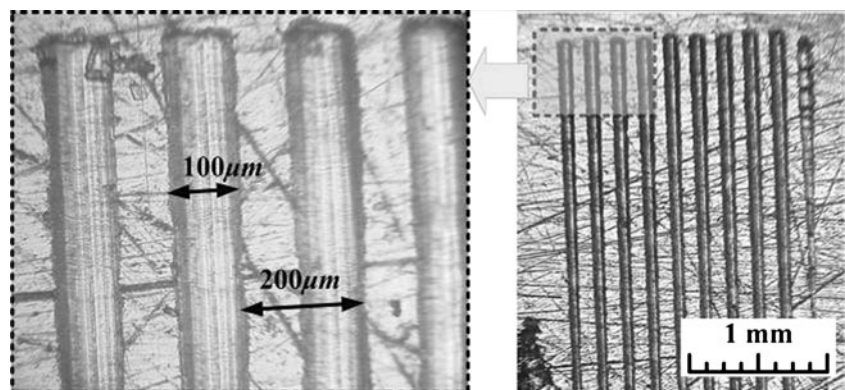
Table 2 Cutting parameters (AL 2024)

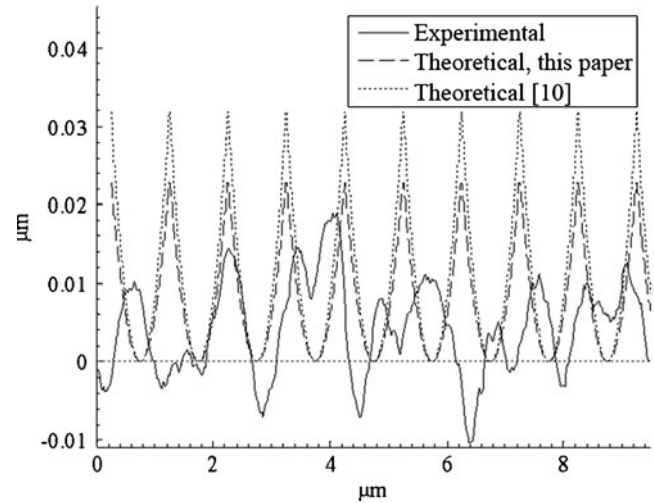| Property	Value	Unit
Axial vibration amplitude	5	μm
Transverse vibration amplitude	5	μm
Vibration frequency	100	Hz
In line feed rate	6	mm/min
Crossfeed rate	200	μm/pass
Depth of cut	3	μm

input to APEX PA85 amplifier circuit which is capable of driving high voltage instruments such as the SCMAR. The setup used in implementing the BUEVA is shown in Fig. 10 which includes the following pieces of equipment and functional modules:

- BUEVA
- Haas five-axis vertical machining center
- BUEVA driver (amplifier for driving the SCMARs)
- Kistler 9254 three-axis dynamometer
- Kistler 5070 multichannel charge amplifier
- Oscilloscopes
- PC1 (Kistler DynoWare to log cutting forces)
- PC2 (function generator for the BUEVA driver)
- NI DAQ AT-MIO-16DE-10 (output the driving signal)
- NI DAQPad-6020E (output terminal)

Fig. 17 Inline surface roughness for cutting tests (in Al2024) corresponding to Table 2

Figure 11 illustrates the connectivity of the various modules and components shown in Fig. 10. From the tool side, the BUEVA is fixed on the spindle of the Haas VF6 machining center to generate the required tool path. Wires extend from the BUEVA to the outputs of the driver which takes its driving inputs from the DAQ. The workpiece on the other hand is fixed on the Kistler table dynamometer which is connected to the 5070 multichannel charge

Fig. 16 Experimental versus theoretical force components for Al2024 cutting tests corresponding to Table 2 (*left*: thrust force; *right*: cutting force)
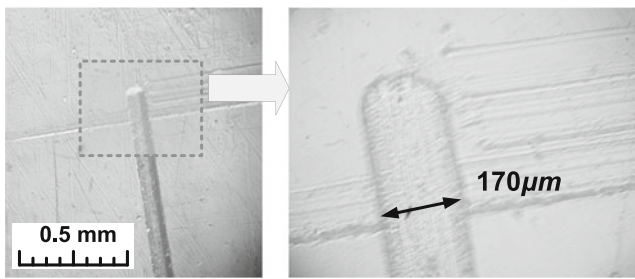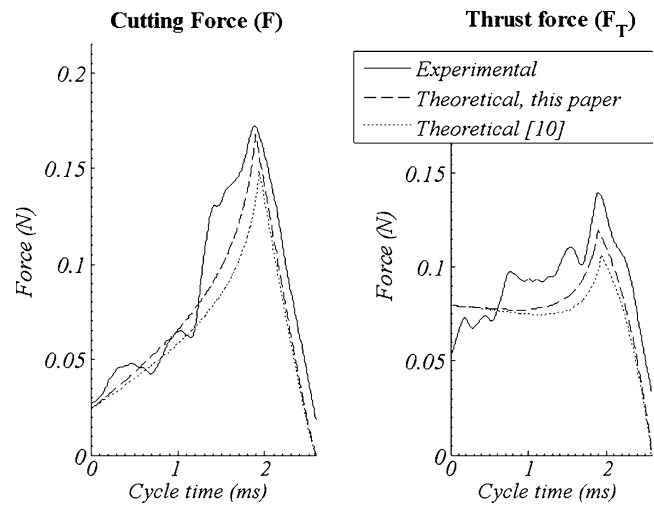
Fig. 18 A photograph of 170-μm-wide groove in plexiglas corresponding to Table 3

Fig. 19 Calculated versus measured force components for cutting tests (in Plexiglas) corresponding to Table 3

amplifier. The signal from the charge amplifier is delivered to PC1 where Kistler DynoWare transforms the electrical signal to force readouts. Driving the actuator is done from the other PC by a LabVIEW VI which serves as a function generator. The desired control parameters (frequency and amplitude of vibration) are input to VI which transforms it to electrical driving signals. The LabVIEW VI module takes into consideration the preload of each SCMAR and its operating voltage to output the correct driving voltages that correspond to the desired input. These outputs are transferred by a NI DAQ AT-MIO to the BUEVA driver which controls the actuator.

The flowchart diagram in Fig. 12 shows the flow of inputs and outputs of the system as well as the overall scheme. Currently, BUEVA's control scheme is open loop meaning that there is no feedback from the tool side to provide information about the tool motion during cutting. The consequence of such control scheme will show in the surface roughness of the machined workpiece (as will be seen below). If the cutting force exceeds the blocking force of the SCMAR, or if undesired vibration from the tool side occurs, the tool will not follow the prescribed elliptical path and thus deterioration in the surface roughness will occur. However, since piezo stacks are being used, this may occur only if undesired external vibrations were to occur (which was not observed in this work). The actuator system's resulting operating parameters are summarized in Table 1.

Table 3 Plexiglas cutting parameters

Property	Value	Unit
Axial vibration amplitude	5	μm
Transverse vibration amplitude	10	μm
Vibration frequency	100	Hz
In line feed rate	6	mm/min
Crossfeed rate	0	μm/pass
Depth of cut	0	μm

4 Evaluation cutting tests

BUEVA performance was evaluated by performing several cutting tests on two different materials: AL2024 and Plexiglas.

4.1 Cuts in Al 2024

Rectangular surfaces were also machined by cutting several proximal straight grooves at a 50-μm pitch in AL2024 (Fig. 13). The resulting crossfeed surface roughness shown in Fig. 14 (corresponding to Fig. 13) was collected using AMBiOS XP1 profilometer. The results show the consistency in consecutive cutting paths.
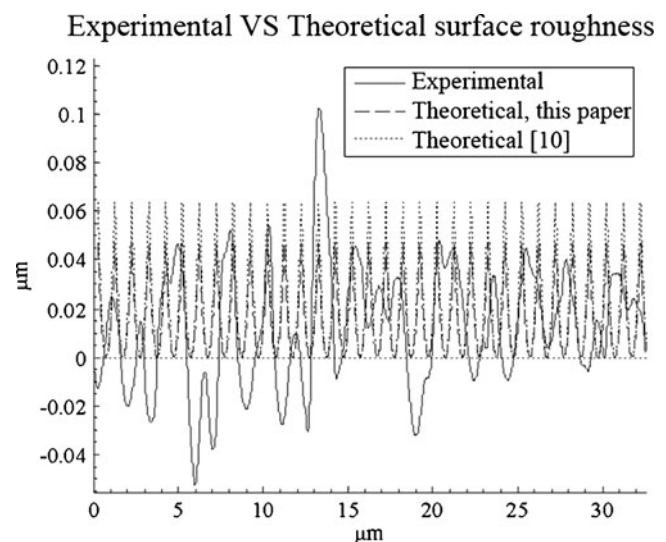
Fig. 20 Inline surface roughness for cutting tests (in Plexiglas) corresponding to Table 3

For further validation, 100-μm-wide parallel grooves were patterned at 200-μm pitch also in AL2024 as shown in Fig. 15. The cutting parameters of this verification test are as shown in Table 2.

The generated cutting forces were experimentally measured using a three-component Kistler dynamometer (MiniDyn Type 9256C capable of measuring small forces up to 250 N). Theoretical and experimental force profiles are contrasted components for a typical cut in Al2024 in Fig. 16 (left: cutting force; right: thrust force). The figure clearly shows the impact of the improvement resulting in a more accurate chip geometry estimate. The "ideal" cutting forces model calculations (MATLAB) fit the experimental force measurements better than when using the reference theoretical forces based on the work by Cerniway [10].

The inline surface roughness generated by the first test showed a maximum surface roughness of 0.0295 μm compared to the 0.0228 μm theoretical value (this work) and 0.0325 (according to [10]). The improved model in this work generated a more accurate surface roughness that is predicted in [10]. The resulting surface roughness error (27%) in our experimental surface roughness is likely caused by the open-loop control of the SCMAR that causes the tool sometimes to produce undesirable vibrations thus deviating from the elliptical cutting path and causing the workpiece surface to deteriorate sometimes. Figure 17 shows a plot of surface metrology measurements relevant to the cuts in Fig. 15. The plot contrasts the experimental roughness profile (AMBiOS XP1 Profilometer) versus ideal surface calculations generated according to the approach outlined in Section 2 above (calculations were done using MATLAB). Also co-plotted are reference theoretical roughness predictions as reported by Cerniway [10].

4.2 Cuts in Plexiglas

A Plexiglas specimen was also used to validate the capability of BUEVA to cut in plastic material. The choice of Plexiglas was due to its transparent property that renders it useful for the application of microchannels. The inline surface roughness generated from cutting straight grooves of 170 μm width (Fig. 18) in Plexiglas is according to the cutting parameters in Table 3

Figure 19 (left: cutting force; right: thrust force) presents the theoretical and experimental force profiles are contrasted for the Plexiglas cutting tests cut according to the parameters in Table 3. The figure illustrates the improvements in the predicted cutting forces in this work as compared to the reference model utilized in [10].

The theoretical vs. experimental surface roughness comparison for the above cut in Plexiglas is shown in Fig. 20. These cuts resulted in a maximum surface roughness of 0.15 μm compared with a theoretical value of 0.05 μm. This amplitude deviation from the cutting profile is perhaps due to the open-loop control. Another factor may be due, as one may expect, to the ductile cutting mode of Plexiglas.

5 Summary

In this paper, a bi-directional ultrasonic elliptical vibration actuator (BUEVA) which features a novel actuator design is introduced. Some of the salient features of this design include:

– Utilization of a vertical tool orientation
– Use of piezo stacks to generate a stiff elliptical path
– Ability to vary the vibration frequency according to the material being cut
– Utilization of an off the shelf TiALN-coated carbide lathe cutting tool.

For validation purposes, BUEVA was utilized to fabricate micro channels (grooves) with different profiles in two different materials: Al2024 and Plexiglas. Machining forces (cutting and trust) were experimentally measured using a three-axis mini dynamometer with the results comparing favorably to calculated "ideal" force profiles. Furthermore, surface roughness measurements of these grooved structures were characterized using profilometry techniques the results of which also exhibiting good fairly good agreement with numerical calculations. Both of these accomplishments reflect on the quality of the refined method developed in this work (as compared with other existing models [10, 22]) for estimating chip geometry and area from the knowledge of tool path.

References

1. Dornfeld D, Min S, Takeuchi Y (2006) Recent advances in mechanical micromachining. CIRP Annals—Manuf Technol 55 (2):745–768
2. Sawada K, Kawai T, Takeuchi Y, Sata T (2000) Development of ultraprecision micro grooving (manufacture of V-shaped groove). SME Int J Series C: Mech Syst Mach Elem Manuf 43(1):170–176
3. Suzuki N, Nakamura A, Shamoto E, Harada K, Matsuo M, Osada M (2003) Ultraprecision micromachining of hardened steel by applying ultrasonic elliptical vibration cutting. Proceedings of 2003 International Symposium on Micromechatronics and Human Science, 221–6
4. Moriwaki T, Shamoto E (1991) Ultraprecision diamond turning of stainless steel by applying ultrasonic vibration. CIRP Annals - Manuf Technol 40(1):559–562

Int J Adv Manuf Technol (2012) 58:991–1001
1001

5. Moriwaki T, Shamoto E (1992) Ultraprecision ductile cutting of glass by applying ultrasonic vibration. Annals of CIRP 41(1):35–38
6. Wang X, Zhou M, Gan J, Ngoi B (2002) Theoretical and experimental studies of ultraprecision machining of brittle materials with ultrasonic vibration. Int J Adv Manuf Technol 20(2):99–102
7. Yamazaki T, Tsuchiya L, Sato U (2007) Ultrasonic vibration cutting of Ti-6 mass% Al-4 mass% V alloy. J Jpn Inst Light Metals 54(4):152–156
8. Shamoto E, Moriwaki T (1994) Study on elliptical vibration cutting. CIRP Ann 43(1):35–38
9. Moriwaki T, Shamoto E (1995) Ultrasonic elliptical vibration cutting. CIRP Annals - Manuf Technol 44(1):31–34
10. Cerniway M (2001) Elliptical diamond milling: kinematics, force and tool wear. Dissertation, North Carolina State University, Mechanical and Aerospace Engineering Department. Raleigh, NC.
11. Negishi N (2003) Elliptical vibration assisted machining with single crystal diamond Tools. Dissertation, North Carolina State University, Mechanical and Aerospace Engineering Department. Raleigh, NC.
12. Brocato B (2005) Micromachining using elliptical vibration assisted machining (EVAM). Dissertation, North Carolina State University, Mechanical and Aerospace Engineering Department. Raleigh, NC.
13. Suzuki N, Masuda A, Haritani M, Shamoto E (2004) Ultraprecision micromachining of brittle materials by applying ultrasonic elliptical vibration cutting. Proceedings of 2004 International Symposium on Micro-Nanomechatronics and Human Science 133–8
14. Shamoto E, Suzuki N, Tsuchiya E, Hori Y, Inagaki H, Yoshino K (2005) Development of 3 DOF ultrasonic vibration tool for elliptical vibration cutting of sculptured surfaces. CIRP Annals - Manuf Technol 54(1):321–324
15. Shamoto E, Suzuki N, Hino R, Tsuchiya E, Hori Y, Inagaki H, et al. (2005) A new method to machine sculptured surfaces by applying ultrasonic elliptical vibration cutting. Proceedings of 2005 International Symposium on Micro- and Nano-mechatronics for Information-Based Society, 91–6
16. Li X, Zhang D (2006) Ultrasonic elliptical vibration transducer driven by single actuator and its application in precision cutting. J Mater Process Technol 180(1–3):91–95
17. Suzuki N, Yan Z, Hino R, Shamoto E, Hirahara Y, & Masuda T (2006) Ultraprecision micro-machining of single crystal germanium by applying elliptical vibration cutting. 2006 IEEE International Symposium on Micro-Nanomechatronics and Human Science, 6
18. Suzuki N, Haritani M, Yang J, Hino R, Shamoto E (2007) Elliptical vibration cutting of tungsten alloy molds for optical glass parts. CIRP Annals—Manuf Technol 56(1):127–130
19. Ammouri A (2008) Bi-directional ultrasonic actuator for vibration mechanical micro-machining. Dissertation, Mechanical Engineering Department, American University of Beirut, Beirut, Lebanon
20. Kim HS, Kim SI, Lee K, Lee DH, Bang YB, Lee K (2009) Development of a programmable vibration cutting tool for diamond turning of hardened mold steels. Int J Adv Manuf Technol 40:26–40
21. Kim GD, Loh BG (2008) Characteristics of elliptical vibration cutting in micro-V grooving with variations in the elliptical cutting locus and excitation frequency. J Micromec Micro-engineering 18:12
22. Arcona C (1996) Tool Force, Chip Formation and Surface Finish in Diamond Turning. Dissertation, North Carolina State University, Mechanical and Aerospace Engineering Department. Raleigh, NC

Springer